Sampling Rate in the Dynamic Speckle Analysis

Pujaico Rivera, F., Gonzalez-Peña, R. J., Braga, R. A.

University Federal of Lavras, Lavras, Brazil

Abstract

In this article, we show as the variation of sampling rate, in a dynamic speckle analysis, affects the value of some dynamic speckle indexes, to the cases of the absolute value of the differences index, the temporal speckle standard deviation index and the temporal speckle mean index. We show that the dynamic speckle index value changes its maximum excursion with the variation of sampling rate, affected directly by the time integration (exposition time) of camera. We highlight the importance of knowing the frequency band of analyzed phenomenon, in order to choose the appropriate sampling rate, being recommendable to use the minimal sampling rate possible to get an acceptable maximum excursion, and an illumination level with good signal-noise ratio.

Keywords: Sampling rate, Dynamic speckle index, Dynamic speckle index, Dynamic speckle analysis

1. Introduction

The dynamic laser speckle analysis is an important study topic[1, 2, 3, 4, 5] to determine the activity level of biological materials. The importance of technical aspects of dynamic laser speckle analysis, as the stability of laser illumination level has been analyzed [3], and it was analyzed the effect of illumination instability over an index value [3], such as the absolute values of the differences [6, 7]. It was showed the dependence between the index value and the illumination level.

Thus, it is necessary analyze the effect of technical parameters that affect the perceived illumination level; in these sense, we analyze the effect of sampling

rate, and consequently the time exposure, in a dynamic laser speckle analysis that use: the absolute value of the differences index, the temporal speckle standard deviation index and the temporal speckle mean index [8].

Knowing the effect of sampling rate over an index value, a researcher will be able to have a criteria to choose the appropriate sampling rate for a certain monitored phenomenon.

For this purpose, we show that given a dynamic speckle test, exists an appropriate frequency band to the sampling rate. High values of sampling rate may cause unintended consequences on the index value, such as the decrease of the excursion between two activity levels, given a determinate index value. In turn, decreasing the sampling rate promoted by the increasing of the exposure time, will cause a reduction of the temporal speckle contrast, and consequently limit the possibility to get information from the sample.

To be able to demonstrate the existence of this appropriate frequency band, we will perform two types of tests; in the first, we analyzed an ink drying process along the time; and in the second, we tested the activity state of a corn seed, with 3 days of germination. In both cases, were used four different sampling rates, and was compared the behavior of speckle indexes.

In the next section we describe how the speckle images were acquired and the setup used to analyze them; all theoretical definitions, necessary to understand the analysis, will shown in the Section 3; numerical results of the analysis are presented in Section 4, and an analysis of the results is reported in the Section 5; finally, we present our conclusion in the Section 6.

2. System description

2.1. Time exposure of the camera

The sampling rate (F_s) or acquisition time in frames per second (fps), in the camera Marlin F-033 is obtained using the Table 1, where we can see the 4 sampling frequencies that will be used in the tests; these values were obtained using the shutter register value ($Shutter$), the time base register value ($Base$),

$Shutter$	$Base\ [\mu s]$	$Offset\ [\mu s]$	$E\ [ms]$	$F_s\ [fps]$
3332	20	12	66.652	15.003
1665	20	12	33.312	30.019
1110	20	12	22.212	45.021
832	20	12	16.652	60.053

Table 1: Exposition time and sampling rate

the exposure time offset ($Offset$) and the effective exposure time (E); so that the exposure time ($Exposure$),

$$Exposure = Shutter \times Base, \tag{1}$$

$$\frac{1}{F_s} = E = Exposure + Offset. \tag{2}$$

Where, F_s is calculated in relation to E; being that, the $Exposure$ represent the photography integration time and E the effective time between photographs; the difference between these two exposures arise from $Offset$ time, that is the time between end and start of a photography. In all cases the exposure time is much bigger than $Offset$; so, we can approximate that $F_s \approx 1/Exposure$.

2.2. Data-packages of ink drying process

This data set comes from an ink drying process, where groups of images (data package) are taken at the times {0, 1, 2, 3, 4, 5, 6, 7, 8, 9, 10} min. In each time, an acquired package has 512 images of 147 pixels of height and 166 pixels of width. 4 different sampling rates were used to take the images, being these rates 15, 30, 45 and 60 hz.

2.3. Data-package of maize seed germination

This data-package has the speckle pattern of a maize seed with 3 days of germination, where four data-packages with different sampling rates (15, 30, 45 and 60 hz) were built. Each package have 512 images of 15 pixels of height and 15 pixels of width.

2.4. Test 1: ink drying process

Fig. 1 represents the data analysis method in an ink drying process, to a F_s sampling rate. Where, $P(t)$ is an data-package with images at the time t

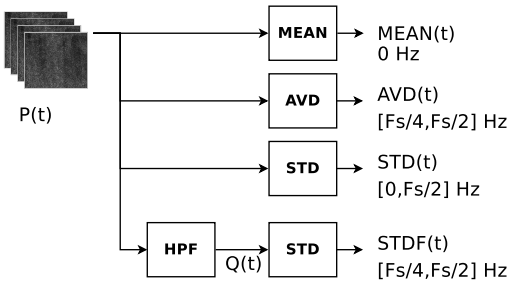

Figure 1: Data analysis of the ink drying process test.

minutes; this package has N images and M pixels; $P_{n,m}(t)$ define the n-th image and m-th pixel, for all $1 \leq n \leq N$, $1 \leq m \leq M$. The $MEAN$ block represents the calculation of temporal speckle mean index on the package $P(t)$, returning the value $MEAN(t)$. The AVD block represents the calculation of absolute values of the differences index on the package $P(t)$, returning the value $AVD(t)$. The STD block represents the calculation of the temporal speckle standard deviation index on the package $P(t)$ or $Q(t)$, returning the value $STD(t)$ or $STDF(t)$, respectively. And finally, the block HPF represents a digital finite impulse response "high-pass filter" with order 40 and cut-off at $0.25F_s$; this block filter the $P(t)$ package and return $Q(t)$, leading this result to a STD block to finally obtain the $STDF(t)$ index value. According to the information of the data packages, we will have speckle indexes values, for each minute, during 10 minutes.

2.5. Test 2: Maize seed germination

The speckle activity of a maize seed was analyzed in a similar way to the ink drying, seen in the Section 2.4, with the difference that only one data-package was taken at the time t, equal to 3 days of germination.

2.6. Test 3: Frequency band activity analysis

The Fig. 2 represents the frequency band analysis method of data package P, acquired with a sampling rate of F_s. This package is the input of many band pass filter (BPF) blocks, described in the Sec 3.5, these band pass filter have cut-off frequencies between $f_1(l)$ and $f_2(l)$, where l indicates the current band, so that $1 \leq l \leq L$; being L the total number of analysis frequency bands; thus, we obtained the R_l package (a filtered version of P). R_l was processed by a σ block, where it is calculated the σ_m value to each pixel in the package R_l, as described in the Sec 3.3. Finally, an image is obtained and it is named as the variable $STDB_l$.

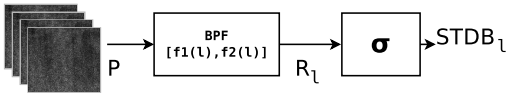

Figure 2: Frequency band analysis of a data package.

3. Theoretical definitions

In the next subsections we use the variable P to define $P(t)$ in any time t; thus, P represents a data collection of images in any time.

3.1. MEAN index

The temporal speckle mean index (μ_m) [8] gives the mean value of the illumination level to the m-th pixel in the package P, and it was implemented as presented in Eq. 3, where N is the number of image in the package,

$$\mu_m = \sum_{n=1}^{N} \frac{P_{n,m}}{N}. \tag{3}$$

Finally, the $MEAN(t)$ index is the spatial mean value of all μ_m results, as can be viewed in the Eq. 4,

$$MEAN(t) = \sum_{m=1}^{M} \frac{\mu_m}{M}. \tag{4}$$

3.2. AVD index

The Absolute Values of the Differences (AVD_m) [6, 7] gives the mean value of the absolute differences in the illumination level of the m-th pixel in the package P, it was implemented by Eq. 5,

$$AVD_m = \sum_{n=2}^{N} \frac{|P_{n,m} - P_{n-1,m}|}{N}. \tag{5}$$

Finally, the $AVD(t)$ index is the spatial mean value of all AVD_m results, as can be viewed in the Eq. 6,

$$AVD(t) = \sum_{m=1}^{M} \frac{AVD_m}{M} \tag{6}$$

3.3. STD index

The temporal speckle standard deviation index (σ_m) [8] gives the standard deviation value of the illumination level to the m-th pixel in the package P, it was implemented with the Eq. 7,

$$\sigma_m^2 = \sum_{n=1}^{N} \frac{(P_{n,m} - \mu_m)^2}{N}. \tag{7}$$

Finally, the $STD(t)$ index is the spatial mean value of all σ_m results, as can be viewed in the Eq. 8,

$$STD(t) = \sum_{m=1}^{M} \frac{\sigma_m}{M} \tag{8}$$

3.4. HPF block

The high-pass filter (HPF) block was implemented (Fig. 1) with a finite impulse response (FIR)[9] filter of order 40 and cut-off at $0.25F_s$. The 41 values in the filter are represented with $h(i)$, for all $0 \leq i \leq 40$, with zero in others cases. Thus, a data package P as input of the HPF block gives us as result, a data package Q, as can be seen in the Eq. 9,

$$Q_{n,m} = \sum_{k=1}^{N} P_{k,m} h(n - k + 20). \tag{9}$$

3.5. BPF block

The band-pass filter (BPF) block is implemented (Fig. 2) similarly as the HPF block, with a FIR filter of order 40 but with a cut-off in $f_1(l)$ and $f_2(l)$,

$$[f_1(l),\ f_2(l)] = \left[\frac{(l-1)}{L},\ \frac{l}{L}\right]\frac{F_s}{2}, \tag{10}$$

representing l, for all $1 \leq l \leq L$, the l-th band of L bands; each band has $\frac{F_s}{2L}$ Hz. The filter is represented with $g(i)$, for all $0 \leq i \leq 40$, with zero in others cases. Thus, a data package P as input of the BPF block gives us as result, a data package R, as can be seen in the Eq. 11,

$$R_{n,m} = \sum_{k=1}^{N} P_{k,m}\ g(n-k+20). \tag{11}$$

4. Numerical results

4.1. Test 1: ink drying process

This test shows the analysis result of an ink drying process, during 10 minutes, using the sampling rates: 15, 30, 45 and 60Hz.

Figure 3 presents the $MEAN(t)$ index, in the test showed in the Section 2.4, to each time t for the 4 sampling rates. It can be seen that, the value of index

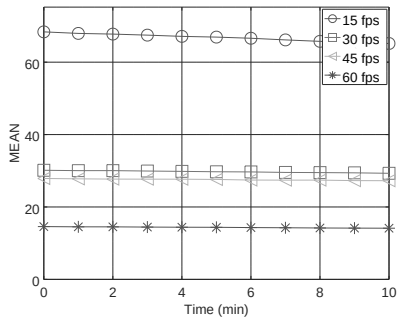

Figure 3: $MEAN$ index value.

has a monotonous behavior over time. By other side the values in the curves decreases in proportion with the grow of sampling rate.

Figure 4 shows the result of analysis explained in the Section 2.4 about the $AVD(t)$ index. The Figure 4a shows the $AVD(t)$ index, in each time t, to

(a) AVD index value. (b) Normalized AVD index value.

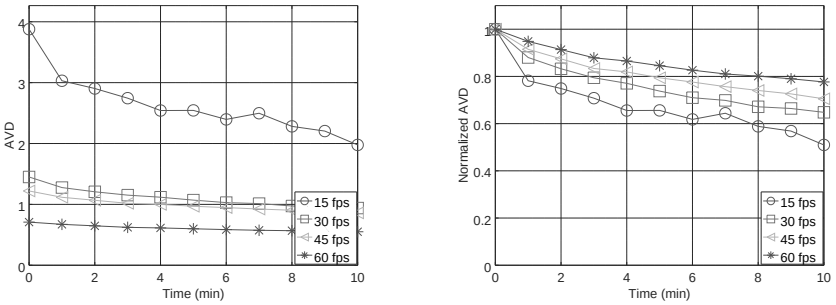

Figure 4: AVD index anaysis.

4 sampling rates, showing a different behavior in time to each sampling rate, so that, the value of the index in all curves, decreases in proportion with the grow of sampling rate. By other side, Figure 4b shows a normalized version of $AVD(t)$ index, so that the maximum value of curves have an unit value; thus, it can be seen that, the maximum excursion of the curve is greatest when the sampling rate decrease. Remembering that this index uses information from a frequency band between $F_s/4$ until $F_s/2$ Hz [7].

Figure 5 presents the $STD(t)$ index in the test showed in the Section 2.4. The Figure 5a shows the behavior of $STD(t)$ index, in each time t, to 4 different sampling rates. Remembering that this index uses information in the entire frequency band (0 until $F_s/2$ Hz), as seen in Section 3.3. This index shows a different behavior in time to each sampling rate, so that, the value of the index in each time decreases in proportion with the grow of sampling rate. By other side, Figure 5b shows a normalized version of $STD(t)$ index; being the unit, the maximum value of curves; thus, it can be seen that exists a small difference between the maximum excursion of the curves with different sampling rates; even so, it is possible to observe a slight decrease of the maximum excursion in

(a) STD index value.

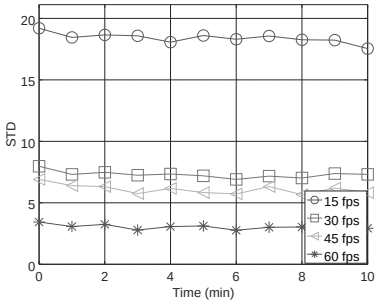

(b) Normalized STD index value.

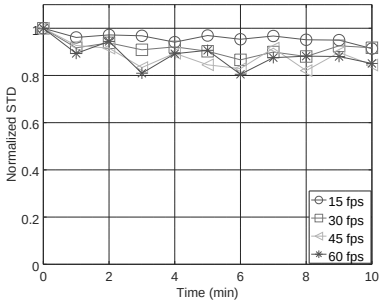

Figure 5: STD index anaysis.

the curve with the grow of the sampling rate, unlike the $AVD(t)$ index.

Figure 6, presents the $STDF(t)$ index, in the test showed in the Section 2.4. Figure 6a shows the behavior $STDF(t)$ index, in each time t, to 4 different sam-

(a) $STDF$ index value.

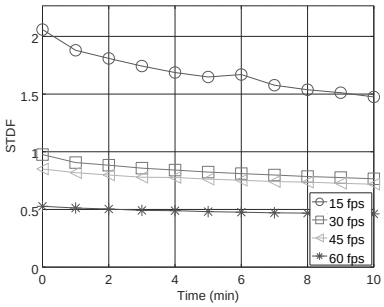

(b) Normalized $STDF$ index value.

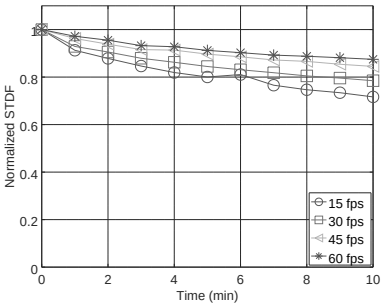

Figure 6: $STDF$ index anaysis.

pling rates. Remembering that this index uses filtered information of datapack, so that the frequency band is between $F_s/4$ and $F_s/2$ Hz. This index shows monotone decreasing behavior in time, where we observe a different behavior in time to each different sampling rate; so that, the value of the index in each time

decreases in proportion with the grow of sampling rate. By other side, Figure 6b shows a normalized version of $STDF(t)$ index; being the unit, the maximum value of curves; thus, it can be seen that exists a considerable difference between the maximum excursion of the curves with the use of sampling rate; so, it is possible to observe a grow of the maximum excursion when the sampling rate decrease, like the $AVD(t)$ index.

4.2. Test 2: maize seed germination

This test shows the result of analyze a corn seed with 3 days of germination, the images were taken using the sampling rates: 15, 30, 45 and 60Hz.

Figure 7 shows the $MEAN(t)$ index, decreasing its value with the increment

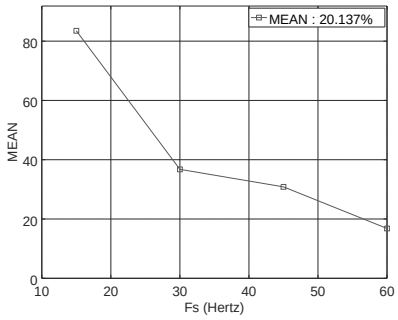

Figure 7: $MEAN$ index value in the germinated corn seed.

of sampling rate, where from 15 Hz to 60 Hz, the index value reached the 20.137% of its value.

Figure 8 shows the $AVD(t)$, $STD(t)$ and $STDF(t)$ indexes, with the same behavior that the presented by $MEAN$ index. The decreasing of the activity observed are related to the increase of F_s where STD, AVD and $STDF$ presented respectively degrowth values of 22.2426% 19.2578% and 20.3541%.

4.3. Test 3: frequency band activity analysis

Table 2 shows the $STDB$ image in different frequency bands of maize seed, using 4 different sampling rates: 15, 30, 45 and 60 Hz, as can be seen in the first column of the table.

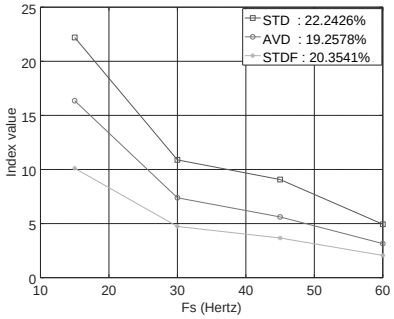

Figure 8: $AVD(t)$, $STD(t)$ and $STDF(t)$ indexes values in the germinated maize seed.

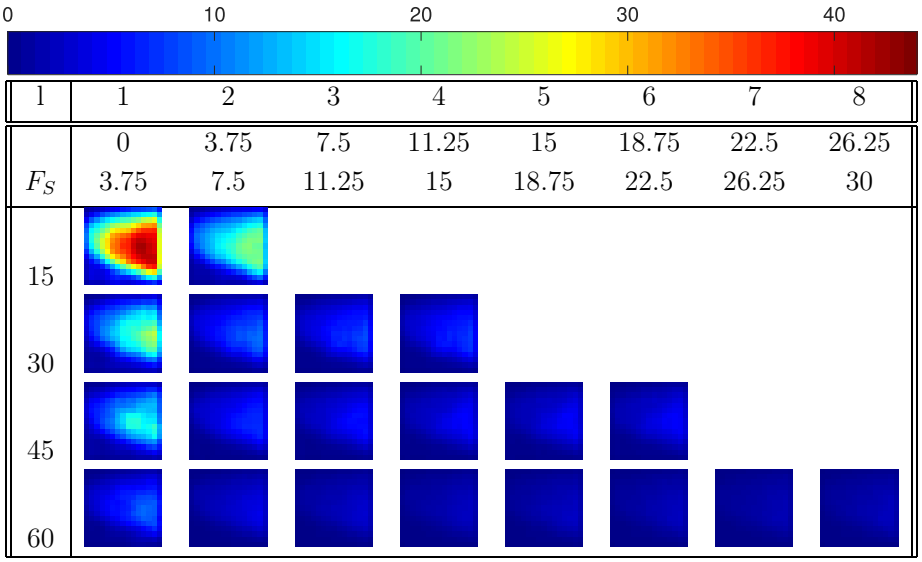

l	1	2	3	4	5	6	7	8
	0	3.75	7.5	11.25	15	18.75	22.5	26.25
F_S	3.75	7.5	11.25	15	18.75	22.5	26.25	30
15								
30								
45								
60								

Table 2: frequency band analysis

In the other columns, we can see the results of 8 frequency bands of package P, represented in the first line of table, with l, that indicates the position of frequency band in crescent order, relative to its frequency components, with limits assigned at the frequencies: 0, 3.75, 7.5, 11.25, 15, 18.75, 22.5, 26.25 and 30Hz; as can be seen in the second line of table. So that, the package sampled at 15hz was divided in $L = 2$ frequency bands, the package sampled at 30hz was divided in $L = 4$ frequency bands, the package sampled at 45hz was divided in

$L = 6$ frequency bands and finally the package sampled at 60hz was divided in $L = 8$ frequency bands.

The matrices $STDB$ are represented using a color palette, that goes from dark blue (low values) to dark red color (high values), linked to the values of activity, it is evident how the index values decreases with the increment of sampling rate F_s. The index values also decrease with the increment of the position of frequency band, being a frequency band between 0 Hz and 3.75 Hz with a sampling rate of 15 hz, the better analysis's case; in the sense of better differentiating places of lower and higher index value.

5. Discussions

In the Figure 3 and 7, the indexes show a relation between the profile of mean index curve and the sampling rate of datapack. The temporal speckle mean index (Fig. 3) is related to the observed illumination level in the surface of the material [8] and correspond to the analysis of zero frequency components of signal. Thus, we can conclude that the level of illumination, perceived by the camera, decrease with the increment of sampling rate. This is because that the exposition time is modified with the alteration of sampling frequency to commercial cameras, so that less lighting is used to take the picture and consequently the temporal speckle mean index decrease in its value. In this sense, it is important to be aware to choose a sampling rate that gives us an index value superior to the noise level of test or to the quantization level of the camera.

The modification of exposition time also affects and limits other indexes, remember that we have a quantization level between 0 and 255 in the camera. We can see this interference in the Figures 4, 5, 6 and 8, where the $AVD(t)$, $STD(t)$ and $STDF(t)$ indexes decrease their values in concordance with the decrease of exposition time. Other way in that the sampling rate affects the values of indexes, can be seen in the limitation of the frequency band of an analyzed signal; for example, a sampling rate F_s, by the Nyquist theorem [10,

11], causes the limitation of frequency band between $0Hz$ and $F_s/2\ Hz$. Thus, in this context we have an index as $STD(t)$ that uses information between $\langle 0, F_s/2]\, Hz$, while other indexes as the $AVD(t)$ and the $STDF(t)$ index, use information of half frequency band, between $[F_s/4, F_s/2]\, Hz$. In the comparison between $STD(t)$ vs { $STDF(t)$ and $AVD(t)$ }, we can see how the use of half, of entire frequency band, causes the decrease in the values of the curves, but give us considerably good values in the maximum excursion of the curve across the time. By other side, in the case of ink drying process, the use of complete frequency band ($STD(t)$ index), it returns low values of maximum excursion in the curves across the time. The importance of excursion, in this test, is due to the need of significant differences between the values of two states, during the drying process.

It is necessary to highlight the importance of to choose the best value of sampling rate F_s; so that, the frequency band of a signal contain the frequency components with the information that you want to analyze; so that, the values of indexes have the greatest values and probably a good excursion, when compared with an inert part of the sample. By example, in the Table. 2, it is analyzed a corn seed, where we can see the major values of indexes are obtained from 0 Hz and 7.5 Hz, when $F_s = 15$ Hz.

Thus, at this point, a question is evident: What is the best frequency band? According with the test of corn seed, we see that for all frequency bands, the best range is the one with the components with lowest frequencies; but without forget that given a $STD(t)$ analysis, this index extract information of inner parts of material [8], and this information decreases jointly with the decrease of frequency band, as can be seen when compared the result in the excursion of $STD(t)$, with components in low frequencies, and the excursion of $\{STDF(t)$ and $AVD(t)\}$, with components in high frequencies; so that we need to choose a compromise between the desired quantity of inner information in the sample, the perceived illumination level and the sampling rate.

6. Conclusion

In this work were presented comparisons of three dynamic laser speckle indexes, subject to different values of sampling rate. thus we conclude that it is important to choose an appropriate sampling rate, being recommendable to use the minimal sampling rate possible to get an acceptable maximum excursion, in index as the AVD and $STDF$, and an illumination level in the images with good signal-noise relation, so that the phenomenon under study can be collected in the chosen analysis frequency band. We showed that the digitization of speckle signal imply a restriction of frequency band of signal and consequently this affect the result of an speckle analysis. And the user of a digital camera must be aware that the increase of the frame rate (fps) force the commercial cameras to change the perceived illumination level in the camera sensor.

7. Acknowledgment

We wish to acknowledge the partial financial support for this study provided by the $CAPES$ scholarship $PNPD$ Program, $FAPEMIG$ and $CNPQ$.

8. Bibliography

[1] M. D. Catalano, F. P. Rivera, R. A. Braga, Viability of biospeckle laser in mobile devices, Optikdoi:10.1016/j.ijleo.2019.02.055.

[2] F. P. Rivera, R. A. Braga Jr, P. Iannetta, P. Toorop, Sound as a qualitative index of speckle laser to monitor biological systems, Computers and Electronics in Agriculture 158 (2019) 271–277. doi:10.1016/j.compag.2019.01.051.

[3] R. J. González-Peña, R. A. Braga Jr, F. Pujaico-Rivera, Diode laser reliability in dynamic laser speckle application: Stability and signal to noise ratio, Optics & Laser Technology 108 (2018) 279–286. doi:10.1016/j.optlastec.2018.07.006.

[4] S. H. Silva, A. M. T. Lago, F. P. Rivera, M. E. T. Prado, R. A. Braga, J. V. de Resende, Measurement of water activities of foods at different temperatures using biospeckle laser, Journal of Food Measurement and Characterization 12 (3) (2018) 2230–2239. doi:10.1007/s11694-018-9839-8.

[5] R. A. Braga, R. J. González-Peña, D. C. Viana, F. P. Rivera, Dynamic laser speckle analyzed considering inhomogeneities in the biological sample, Journal of biomedical optics 22 (4) (2017) 045010. doi:10.1117/1.JBO.22.4.045010.

[6] R. Cardoso, R. Braga, Enhancement of the robustness on dynamic speckle laser numerical analysis, Optics and Lasers in Engineering 63 (2014) 19–24. doi:10.1016/j.optlaseng.2014.06.004.

[7] F. P. Rivera, R. A. Braga Jr, Selection of statistical indices in the biospeckle laser analysis regarding filtering actions, Optics Communications 394 (2017) 144–151. doi:10.1016/j.optcom.2017.03.015.

[8] R. Nothdurft, G. Yao, Imaging obscured subsurface inhomogeneity using laser speckle, Opt. Express 13 (25) (2005) 10034–10039. doi:10.1364/OPEX.13.010034.

[9] T. Saramäki, S. Mitra, J. Kaiser, Finite impulse response filter design, Handbook for digital signal processing 4 (1993) 155–277.

[10] H. Nyquist, Certain topics in telegraph transmission theory, Transactions of the American Institute of Electrical Engineers 47 (2) (1928) 617–644. doi:10.1109/T-AIEE.1928.5055024.

[11] C. E. Shannon, Communication in the presence of noise, Proceedings of the IRE 37 (1) (1949) 10–21. doi:10.1109/JRPROC.1949.232969.